Effects of Bilayer Surface Charge Density on Molecular Adsorption and Transport across Liposome Bilayers

Yan Liu, Elsa C. Y. Yan, and Kenneth B. Eisenthal
Department of Chemistry, Columbia University, New York, New York 10027 USA

ABSTRACT Second harmonic generation (SHG) was used to study both the adsorption of malachite green (MG), a positively charged organic dye, onto liposomes of different lipid compositions, and the transport kinetics of MG across the liposome bilayer in real time. We found that the dye adsorption increased linearly with the fraction of negatively charged lipids in the bilayer. Similarly, the transport rate constant for crossing the bilayer increased linearly with the fraction of charged lipid in the bilayer.

INTRODUCTION

Liposomes are widely used as models of biomembranes and in applications such as solar energy conversion, chemical catalysis, and drug delivery (Gennis, 1989; Lasic, 1993). In all these applications, molecular adsorption and transport kinetics across liposome bilayers play an important role. In this study, we apply a surface technique, second harmonic generation (SHG), to investigate the effect of lipid composition on the adsorption and transport processes. It is demonstrated that the adsorption free energy, the absolute number of adsorbates, and the real-time transport kinetics can be obtained by the SHG method. The adsorbing molecule used in these studies is the triphenyl organic cation, malachite green (MG), which has a charge of +1 (Scheme 1). Different ratios of negatively charged palmitoyloleoyl-phosphatidylglycerol (POPG) and zwitterionic palmitoyloleoyl-phosphatidylcholine (POPC) were used to constitute the liposomes. We found that the higher the fraction of the negatively charged POPG component, the faster the transport rate and the larger the adsorption. We also found that both the number of adsorbates and the transport rate (s^{-1}) scale linearly with the fraction of negatively charged lipid in the liposomes.

Both POPG and POPC have a saturated 16-carbon chain (16:0) and an unsaturated 18-carbon chain with one double bond in between the 9th and the 10th carbon (18:1, 9). This chain structure is the best representative of the lipid structure of lecithins from eggs (Gennis, 1989). The two lipids mix ideally at room temperature (Marsh, 1990), and the transition temperature from gel phase to liquid crystalline phase is at −4°C. Large unilamellar liposomes of submicron size were made by the extrusion method. The surface charge density can be varied by changing the negatively charged POPG content in the liposomes.

A variety of methods, including NMR (Buster et al., 1988; Xiang and Anderson, 1997), EPR spin labels (Cafiso and Hubbell, 1983; Cafiso, 1989; Wallach and Winzler, 1974), fluorescence (Wallach and Winzler, 1974; Eidelman and Cabantchik, 1989), and absorbance (Wallach and Winzler, 1974; Kaiser and Hoffmann, 1996), have been used to study the adsorption onto and the transport across bilayer structures. For charged molecules, including some peptides (Kim et al., 1991; Mosior and McLaughlin, 1991, 1992; Gabev et al., 1989; Chakrabarti et al., 1994), proteins (Zucker et al., 1995; Noy et al., 1992; Kakinoki et al., 1995; Malmstein, 1995; Casals et al., 1993), and drugs (Terce et al., 1982; Aubard et al., 1990; Voelker and Smejtek, 1996), it was found that the electrostatic interaction is the major driving force for the adsorption onto charged liposomes. Studies showed that charged peptides did not adsorb on neutral liposomes composed only of PC lipids, but adsorbed on liposomes composed of a mixture of PC and some charged lipids, such as phosphatidylglycerol (PG), phosphatidylserine (PS), and phosphatidylamine (PA) (Kim et al., 1991; Mosior and McLaughlin, 1991, 1992; Gabev et al., 1989). There are a few liposome studies on the adsorption and transport of hydrophobic ions, e.g., tetraphenylphosphonium (TPP^+), tetraphenylboron (TPB^-) (Flewelling and Hubbell, 1985a,b; Sundeberg and Hubbell, 1986), oxonol dyes (Bashford et al., 1979; Clarke and Apell, 1989; Clarke, 1991, 1992, 1993), and 1-anilino-8-naphthalenesulfonate (ANS^-) (Haynes and Simkowitz, 1977). It is found that both the adsorption and the transport depend not only on the charge distribution and the hydrophobicity of the organic ions, but also on the properties of the liposomes, including the surface charge density and the fluidity of the bilayers (Chakrabarti et al., 1994).

All the above mentioned techniques provide useful information on the liposome systems but suffer from the inability to directly distinguish the molecules adsorbed on the surfaces of the liposomes from those in the bulk solution. SHG detects only molecules bound to the inner and outer surfaces and is insensitive to the molecules in the bulk media. These other methods are complementary and require very precise calibration of the signal changes with the microenvironment

Received for publication 18 July 2000 and in final form 26 October 2000.
Address reprint requests to Dr. Kenneth B. Eisenthal, Department of Chemistry, Havemeyer Hall MC3107, Columbia University, 3000 Broadway, New York, NY 10027. Tel.: 212-854-3175; Fax: 212-932-1289; E-mail: eisenth@chem.columbia.edu.

0006-3495/01/02/1004/09 $2.00

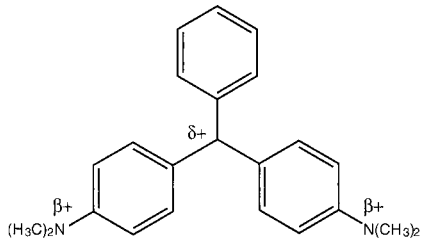

Scheme 1

(NMR line-width broadening, EPR spin labeling), fluorescence, and absorption to separate the surface signal from the huge bulk background signal. Some of the techniques also involve using quenchers and spectral shifting reagents besides the probe molecules, which may perturb the liposome systems. Furthermore, because SHG is a surface technique that is sensitive to both the inner and outer surfaces of the bilayer, there is no need to introduce extraneous probes, quenchers, shift reagents, or other species to differentiate between molecules present in the bulk solution from those adsorbed on the surfaces of the liposomes. The SHG requirement is that the molecule to be studied is non-centrosymmetric. It is an in situ method to probe the molecular adsorption on and transport across liposome bilayers. Moreover, it is sensitive to the molecules bound to the inner and outer surface of liposomes, but not the concentrations in the inner and outer aqueous compartments. Therefore, it can be complementary to the conventional techniques. We have demonstrated that the SHG method can be used to study the molecular transport across liposome bilayers in real time (Srivastava and Eisenthal, 1998; Yan and Eisenthal, 2000) and applied this method to investigate the effect of cholesterol on the molecular transport of MG across dioleoylphosphatidylglycerol liposome bilayers (Yan and Eisenthal, 2000). The present study reports the first application of SHG to investigate the molecular adsorption on liposome surfaces, which yields the adsorption free energy as well as the absolute number of adsorbates on the liposome surfaces.

The second harmonic method

Second harmonic generation (SHG) is a surface-specific technique (Eisenthal, 1996; Corn and Higgins, 1994), which involves the conversion of incident light at a fundamental frequency ω to light at twice the frequency 2ω via a nonlinear interaction with the medium. Under dipole approximation SHG is forbidden in centrosymmetric media, but allowed at non-centrosymmetric interfaces. Recently, SHG has been shown to be a novel technique to probe the interfaces of microscopic particles suspended in liquid media. Because the local regions of the surfaces of microparticles can be non-centrosymmetric even when the microparticle is centrosymmetric, the second harmonic field, E_{SH}, can be generated at the surface upon irradiation with the fundamental light at frequency ω. When the particle size is comparable to the wavelength of the light, the second harmonic fields generated at the surface can be added up coherently and gives a SHG signal. The microscopic particles that have been studied are polystyrene beads (Wang et al., 1996, 1998), oil/water emulsions (Wang et al., 1998; Yan et al., 1998), semiconductor particles (Liu et al., 1999), clay particles (Yan and Eisenthal, 1999), and liposomes (Srivastava and Eisenthal, 1998; Yan and Eisenthal, 2000). Information such as the energetics of the adsorption, the population of molecules at the interface (Wang et al., 1998), the surface potential and charge density at the charged interfaces (Yan et al., 1998), and the spectral properties of the adsorbed species at the interfaces (Liu et al., 1999) have been obtained.

Liposomes are self-assembled, enclosed bilayer structures that separate two aqueous phases. The lipid molecules are arranged in a head-to-tail and tail-to-head geometry across the bilayers. In addition to the outer surface of a liposome in contact with the external aqueous medium, there is an inner surface in contact with the interior aqueous medium (Scheme 2). The thickness of the bilayer is 4–5 nm. When molecules are added externally to the liposomes, a very rapid rise in the SH signal is achieved as the molecules rapidly adsorb onto the outer surface of the liposome. If the liposome is permeable to the molecules, the molecules will migrate across the bilayer and adsorb onto the inner surface. By symmetry, the adsorbed molecules on the inner and outer surface of the liposome are oppositely oriented. Because oppositely oriented molecules are separated by the thickness of the bilayer, 4–5 nm, which is much less than the coherence length of the process, the second-order polarizations generated from the oppositely oriented molecules have opposite phase and cancel. Consequently, the E_{SH} induced from the liposome is proportional to the dif-

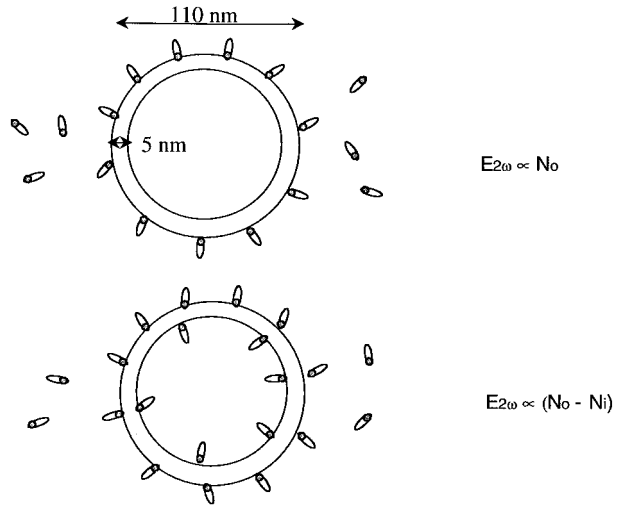

Scheme 2.

ference of the population of the molecules adsorbed on the outer surface, N_o, and the inner surface, N_i:

$$E_{SH}(t) \cong [N_o(t) - N_i(t)] \quad (1)$$

Therefore, by monitoring the SHG signal after the addition of molecules to the liposomes, the transport of molecules from the outer surface to the inner surface can be observed in real time. It is expected that E_{SH} will decrease in time to a finite value rather than zero if the numbers of adsorbed molecules on the inner and outer surfaces differ at equilibrium, due, for example, to the larger surface area of the outer surface and/or electrostatic effects.

MATERIALS AND METHODS

Sample preparation

Large unilamellar liposomes with different mole ratios of POPG to POPC were prepared by the extrusion technique (Hope et al., 1985). The mole percentages of POPG were chosen to be 0, 25, 50, 75, and 100%. A 20-mg amount of the POPG plus POPC dry powders (Avanti Polar Lipids, Alabaster, AL) were weighed into a round bottom flask, then dissolved in 10 ml of chloroform. The solvent was evaporated under vacuum in a rotavapor setup for more than 2 h. The thin film of lipids obtained was hydrated by 10 ml of citrate buffer (ionic strength, 12 mM; pH 4) with vigorous vortexing. The multilamellar liposomes formed were extruded 10 times through doubly stacked 0.2-μm polycarbonate filter under N_2 at pressure 100–120 psi. It had been determined by ^{31}P NMR experiments that more than 90% of the liposomes are unilamellar (Mayer et al., 1986). These stock solutions were stored at 4°C until they were diluted 100 times in the same citrate buffer for the SHG measurements.

The sizes of the liposomes were obtained from UV/VIS turbidity measurements (Engelbert and Lawaczeck, 1985; Kerker, 1970). The liposomes of different compositions were found to be very close in size, ranging from 107 to 112 nm in diameter, except the one composed only of POPC, which was larger than the others (~150 nm).

MG chloride purchased from Aldrich (Milwaukee, WI) was used as received after the purity was checked by HPLC. MG solutions of concentrations varying from 0.2 to 40 μM were made in the same citrate buffer solution. It has an absorption at 427 nm, which is in resonance with the second-harmonic frequency of the fundamental laser input and therefore gives a resonance enhancement of the SHG signal.

For all of the following experiments, the total lipid concentrations after mixing with MG solution are the same, 12.5 μM.

SHG measurement

The setup of the SHG measurements is shown in Fig. 1. Briefly, an argon ion laser pumped Ti:sapphire oscillator yielded 100-fs pulses at 832 nm at a repetition rate of 82 MHz, with an energy of 10 nJ per pulse. After passing through a half-wave plate and a polarizer, the light was gently focused into the sample in a 1-cm rectangular cuvette. The SH photons generated from the sample were collected at an angle of 90° to the incident light by a lens and then focused into the monochromator. A computer connected with the photomultiplier and the single-photon counter was used to record the signal in real time. The SHG measurements were carried out in a 90° geometry. We found experimentally that for small particles (roughly, <0.2 μm), the 90° detection geometry gives a higher SHG signal, whereas for larger particles, (roughly, >0.2 μm), the forward geometry gives a higher SHG signal. We chose the 90° geometry to optimize the SHG signal from the liposome samples, which were ~0.1 μm in diameter.

At room temperature, 22°C, the liposome solution was injected into an equal volume of the MG solution by a syringe. The injections were completed within 1 s. The second harmonic intensity I_{SH} was monitored as a function of time.

RESULTS AND DISCUSSION

Transport kinetics

Fig. 2 shows a typical time profile of the SH intensity before and after a liposome solution was injected into a MG

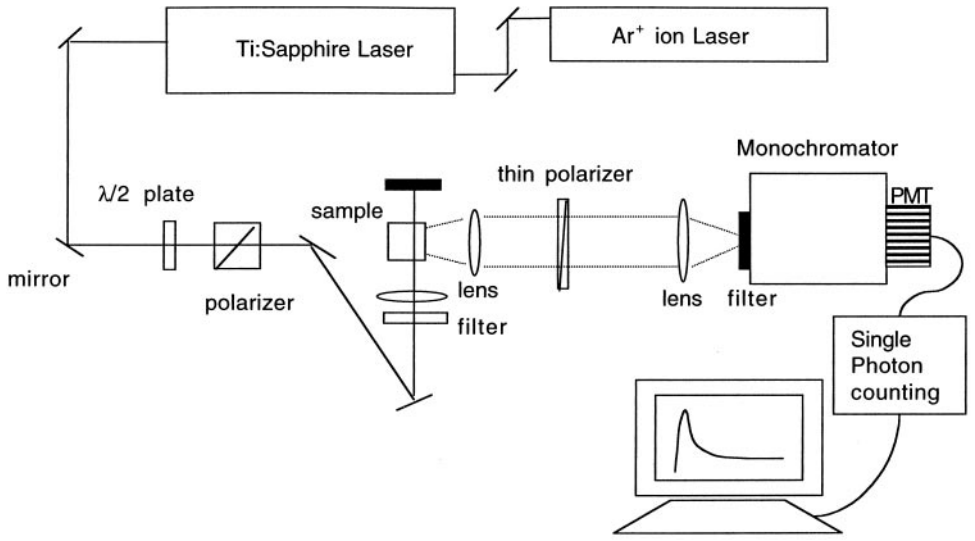

FIGURE 1 Experimental setup for the 90° geometry second harmonic measurement.

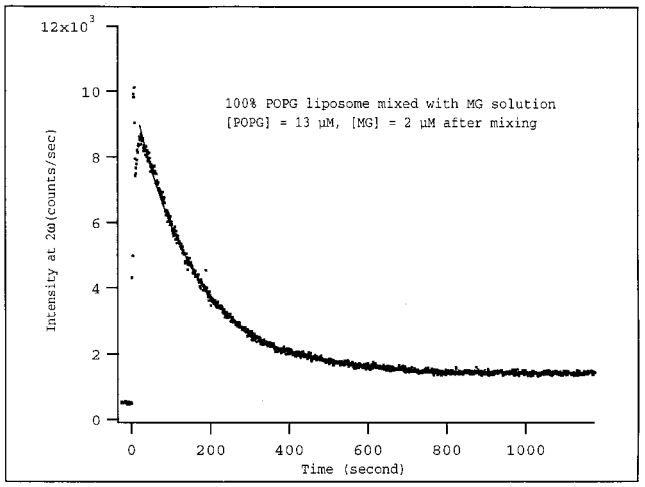

FIGURE 2 A typical decay curve of SHG signal upon injection of liposome into a MG solution. The incident light is at 832 nm, and the signal is recorded at 416 nm. The dots are the data points for 1-s integration time.

solution. The initial signal level is from the MG solution alone, which contains the hyper-Rayleigh scattering of water and the two-photon fluorescence tail of MG. The intensity of the hyper-Rayleigh scattering of water is very low (~20 counts/s) compared with the two-photon fluorescence tail of MG (~50–500 counts/s, in the concentration range of 1–12 μM). We also found that the signal from liposomes in water without MG is comparable to the water alone. The turbidity of the liposomes at the particle density $\sim 10^{10}$ particles/cm^3 was low, and thus the presence of liposomes does not scatter the hyper-Rayleigh of water significantly. The SHG signal increased immediately after a liposome solution was injected, which is due to the adsorption of MG on the outer surface of the liposomes. This observed signal is more than 30 times higher than the MG alone for the liposomes of 100% POPG at 2 μM MG concentration. Following the initial increase of the SHG signal, which is determined by the instrument response time, the signal decreases. The decrease is the result of MG molecules diffusing across the liposome bilayers and adsorbing on the inner surfaces with an orientation opposite to those on the outer surfaces. The nonzero signal at equilibrium is due in part to the different number of adsorbate sites on the inner and outer surfaces and the electrostatic effects due to the buildup of charge at the inner bilayer interface, which lead to an incomplete cancellation of the SHG signal. The nonzero signal level at the long time corresponds to the adsorption equilibrium, which will be discussed in the next section.

It was found that similar time profiles of the SHG, i.e., a rapid rise followed by a slow decay to an equilibrium level, were obtained for all the liposome samples upon mixing with MG solutions except for the liposome sample composed only of zwitterionic POPC. The time profile of the output signal at frequency 2ω for POPC liposomes is shown in Fig. 3. The signal drops to one-half of its original value after the injection of an equal volume of MG solution and then remains at a constant level. The 50% decrease in signal is the result of the dilution of the MG solution upon injecting an equal volume of the liposome solution, i.e., from 40 to 20 μM. This result indicates that the signal observed in Fig. 3 is primarily the two-photon fluorescence of MG, which scales linearly with the MG concentration. We experimentally found that the signal level from 20 μM MG solution with and without the presence of liposomes was the same, which indicates that there is no SHG signal observed from the POPC liposomes with MG. This suggests that MG molecules are not adsorbed on the zwitterionic POPC liposomes.

The SH field, E_{SH}, which is directly proportional to the difference of population on the inner and outer surfaces of liposomes, can be plotted as a function of time. This can be done by the following calculation:

$$E_{SH}(t) = \sqrt{I^{2\omega}_{MG-liposome}(t) - I^{2\omega}_{MG}}, \quad (2)$$

where $I^{2\omega}_{MG\text{-}liposome}(t)$ is the total signal detected at frequency 2ω after injection of the liposome solution into the MG solution at time t, and $I^{2\omega}_{MG}$ is the background signal of the MG solution.

For the liposomes with various POPG contents, the SH decays were obtained for a series of MG concentrations. Fig. 4 *A* shows the decays for 50:50 PC:PG at different concentrations of MG, whereas Fig. 4 *B* shows the decays for the concentration of 8.0 μM MG solution for liposomes with different lipid contents. The SH field decays are fitted to single-exponential functions and both the final signal

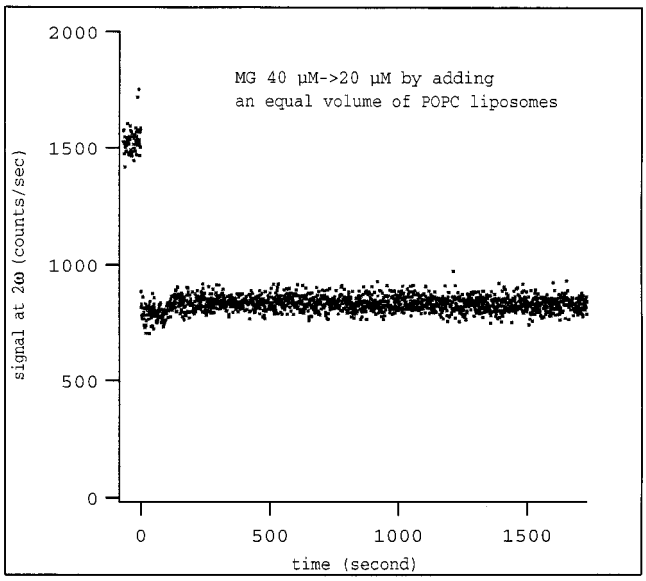

FIGURE 3 Signal intensity upon injecting an equal volume of 100% POPC liposome into MG solution.

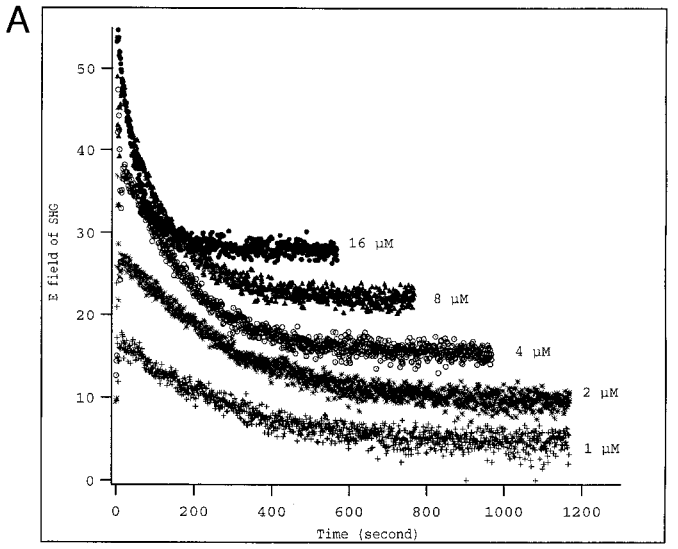

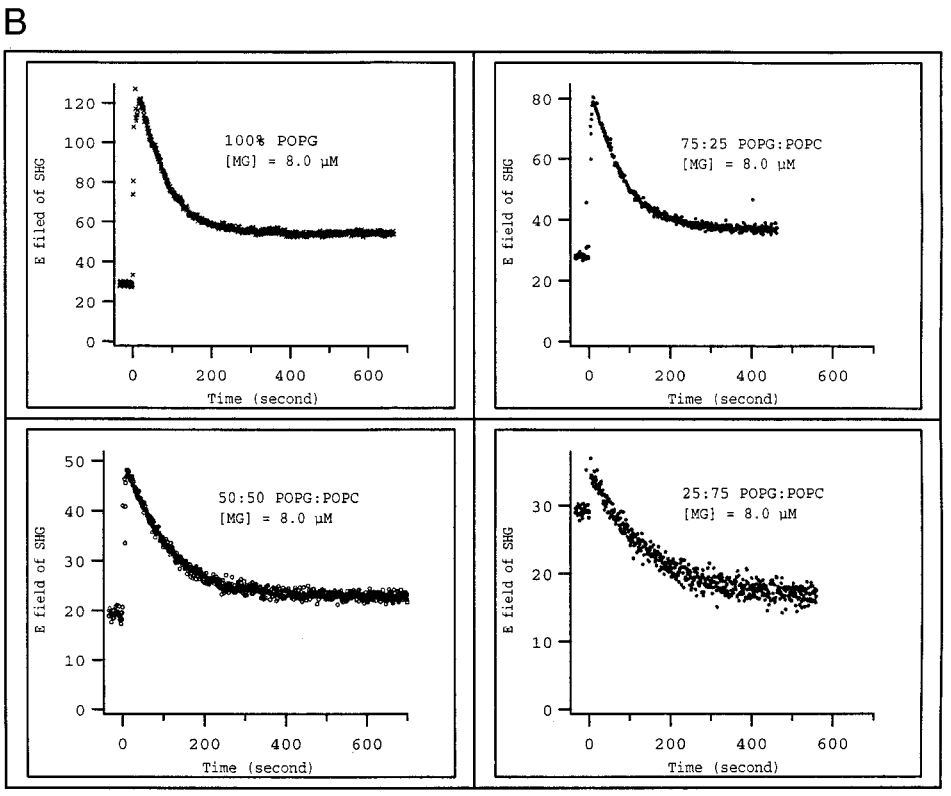

FIGURE 4 (*A*) Decay curves of SHG fields for 50:50 PC:PG liposomes with different MG concentrations. (*B*) Decay curves of SHG fields for liposomes with different lipid contents at the same MG concentration of 8.0 μM. For *A* and *B* the MG fluorescence at 2ω has been subtracted out (Eq. 2).

level and the decay constants are obtained. The final signal level is related to the adsorption equilibrium of MG on the liposome surface, which will be discussed in the next section. The decay constants for different liposomes are plotted as a function of MG concentration (Fig. 5), which all show a linear dependence on the MG concentration. All lines give non-zero intercepts on extrapolation of MG to zero concentration. It is also found that the slopes of these curves, dk/dc, scale linearly with the fraction of negatively charged PG lipids in the liposomes (Fig. 6).

It is to be noted that we empirically fitted the data to a single-exponential function. At low MG concentrations (<10 μM), the fittings were excellent. Fitting these data to a double-exponential function gives two very similar time constants, with negligible improvement in the fitting residue. However, at higher MG concentrations (>12 μM), besides the fast decay (tens of seconds), another decay with a much longer time constant (>1000 s) was observed (data not shown). At this point, we do not have a model that can fully incorporate all of our experimental observations,

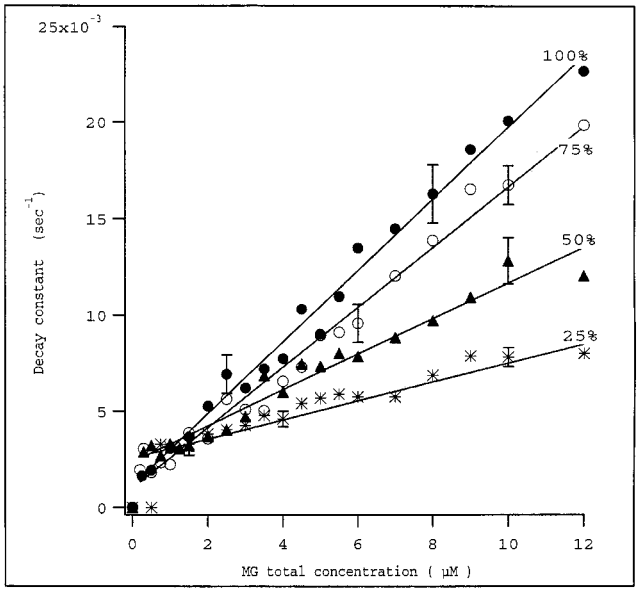

FIGURE 5 The decay constants k (s^{-1}) are linearly dependent on MG concentration for all of the four liposomes.

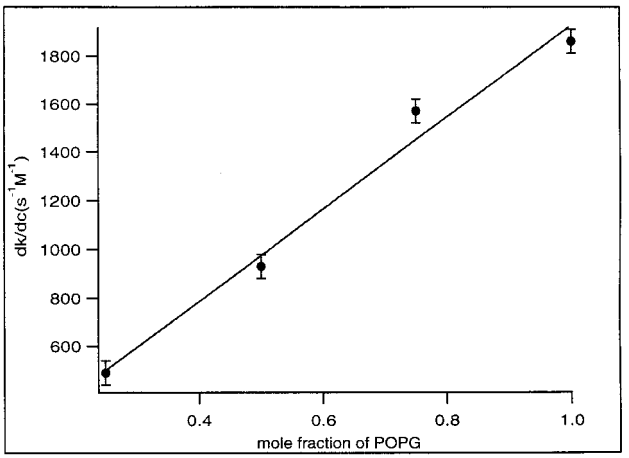

FIGURE 6 The slope of the linear curves dk/dc in Fig. 5 is linearly dependent on the fraction of POPG in the liposomes.

which include 1) the exponential decay of the difference in population on outer and inner surfaces of the liposomes, 2) the linear dependence of the decay constants on MG concentration spanning the whole range of MG concentration (0.2–12 μM), and 3) that the rate constant goes to a nonzero constant as MG concentration goes to zero.

In the literature, there have been a few models to describe the transport of hydrophobic ions across the lipid bilayer (Flewelling and Hubbell, 1985a,b; Sundeberg and Hubbell, 1986; Bashford et al., 1979; Clarke and Apell, 1989; Clarke, 1991, 1992, 1993; Ketterer et al., 1971). In a series of studies the interactions of the hydrophobic anion Oxonol V with neutral 1,2-diacyl-*sn*-glycero-3-phosphocholine (DOPC) vesicles were investigated by a stop-flow fluorescence technique (Clarke and Apell, 1989; Clarke, 1991, 1992, 1993). A three-capacitor model with an application of the Deby-Huckel theory was proposed to describe the experimental data (Clarke, 1993). In the numerical simulation non-exponential transport kinetics was obtained. However, it is also stated that exponential kinetics can be obtained for the case where the dye/vesicle adsorption sites ratio is small. This model predicts the following phenomena: 1) saturation of the binding sites on both inner and outer surfaces of a liposome, 2) the transport rate constant increases as the dye/vesicle ratio increases, and 3) the transport rate constant k (s^{-1}) goes to a non-zero constant as the dye/vesicle ratio goes to zero (i.e., it is the rate constant in the absence of a potential difference across the bilayer). Our observations agree with these predictions. However, this model does not predict a linear dependence of the rate constant on the dye concentration, which we observed in our experiments. In addition, the liposomes used in our experiments were negatively charged due to the presence of POPG whereas the simulations used a neutral liposome of DOPC. In this model simulation, the effects of electrostatic interactions between the surface charges on liposomes and the organic ions are not considered. It is obvious that more needs to be done to fully understand the mechanism of the positively charged MG crossing the negatively charged POPG-POPC liposome bilayers.

Adsorption equilibrium

By measuring the long time values of the SH signal $E_{SH}(c)$ at different MG concentrations, we can obtain the adsorption isotherms for the four samples of liposomes with different POPG content (Fig. 7).

We propose the following model for the adsorption process, including 1) the adsorption of MG molecules from the outer bulk aqueous phase to the outer surface of the liposome and 2) the translocation of the molecules from the outer layer of the liposome to the inner layer of the liposome. The adsorption and desorption process of the molecules on the inner surface was neglected because of the fact that the interior volume of a liposome is very small, $\sim 5 \times 10^{-19}$ L per liposome. It is calculated that only three molecules enclosed in such a tiny volume yields a concentration of 10 μM. Based on our later analysis, it will be shown that the number of MG molecules being adsorbed on the surface of the liposomes is of the order of 10^4 per liposome in the range of MG and liposome concentrations used in these experiments. Thus, the number of molecules in the inner volume do not substantially affect the final equilibrium. The following two steps are used to describe the total adsorption

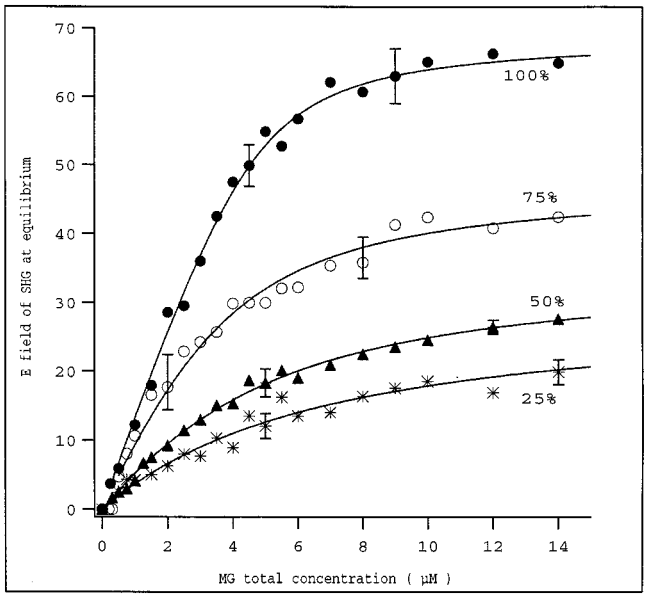

FIGURE 7 The adsorption isotherms of MG on the liposomes with various POPG/POPC ratios. The total lipid concentrations are kept the same in the four cases, at 13 μM.

equilibrium:

$$M + ES_o \overset{K_1}{\rightleftharpoons} FS_o$$

$$FS_o + ES_i \overset{K_2}{\rightleftharpoons} FS_i + ES_o,$$

where M is MG in the bulk solution, ES_o and ES_i are the empty sites on the outer and inner surfaces respectively, and FS_o and FS_i are the filled sites on the outer and inner surfaces respectively. K_1 and K_2 are the equilibrium constants of the two reactions.

In the past, we expressed the equilibrium constants in mole fraction leading to the following expression:

$$K_1 = \frac{55.5\, N_o}{\left[c - \frac{n}{N_A}(N_o + N_i)\right](N_o^{max} - N_o)}, \tag{3}$$

where 55.5 is water molarity, c is the MG bulk concentration, N_o and N_i are the number of MG molecules adsorbed on the outer and inner surfaces of the liposome respectively, N_o^{max} and N_i^{max} are the maximum number of molecules that can be adsorbed at the outer and inner surfaces of the liposome, respectively, n is the number of liposomes per unit volume of the solution, and N_A is Avogadro's number. In Eq. 3, $(n/N_A)(N_o + N_i)$ is the total MG adsorbed onto the surfaces of the liposomes expressed in the unit of concentration (moles per liter). However, we now choose a more conventional standard state of unit concentration, 1 M, as a reference state. Hence, the factor of water molarity of 55.5 in Eq. 3 does not enter. The adsorption free energy can be calculated by

$$\Delta G = -RT \ln K_1, \tag{4}$$

where R and T are the gas constant and the temperature, respectively. Consequently, the difference of the adsorption free energy calculated from equilibrium constants expressed in mole fraction and in the 1 M reference standard state is $-RT \ln 55.5$. At 22°C, it is calculated to be 2.4 kcal/mol. In the following data analysis, the adsorption equilibrium constant is referenced to the standard state of unit concentration.

The equilibrium equation for the transport across the liposome bilayers is

$$K_2 = \frac{N_i(N_o^{max} - N_o)}{N_o(N_i^{max} - N_i)}. \tag{5}$$

To solve for $N_o(c)$ and $N_i(c)$ in terms of K_1, K_2, N_o^{max}, N_i^{max}, and c, we combine Eqs. 3 and 5 and obtain a third-order equation of $N_o(c)$, which can be solved readily. Inserting the expression of $N_o(c)$ back into Eq. 5, both $N_o(c)$ and $N_i(c)$ are obtained. An expression of $[N_o(c) - N_i(c)]$, which is directly proportional to the measured $E_{SH}(c)$ can be obtained in terms of K_1, K_2, N_o^{max}, N_i^{max}, and c.

Fitting the adsorption isotherms for the four liposome samples with the parameters of K_1, K_2, N_o^{max}, and N_i^{max}, we found that the K_2 in all cases is close to 1 to give the best fit, which implies that the two rate constants for MG going inward and outward between the two surfaces of the liposome bilayer are equal. This result is not surprising, because we would expect at equilibrium that these two rate constants be close to each other by symmetry.

With $K_2 = 1$, the third-order equation of $N_o(c)$ can be reduced to a quadratic one, the solution of which depends on only two parameters, C_{max}, and K_1:

$$\frac{N_o(c)}{N_o^{max}} = \frac{(c + C_{max} + K_1^{-1}) - \sqrt{(c + C_{max} + K_1^{-1})^2 - 4C_{max}c}}{2C_{max}}, \tag{6}$$

where $C_{max} = (n/N_A)(N_o^{max} + N_i^{max})$, which is the maximum molar concentration of adsorbates. From Eq. 5, as $K_2 = 1$, $N_i/N_o = N_i^{max}/N_o^{max} = \gamma$. It therefore follows that $E_{SH}(c)$ is directly proportional to $N_o(c)$:

$$E_{SH}(c) \propto [N_o(c) - N_i(c)] \propto (1 - \gamma)N_o(c) \tag{7}$$

It follows that

$$\frac{E_{SHG}(c)}{E_{SHG}^{max}} = \frac{N_o(c) - N_i(c)}{N_o^{max} - N_i^{max}} = \frac{N_o(c)}{N_o^{max}}. \tag{8}$$

Therefore, Eq. 6 can be used to fit the adsorption isotherm with C_{max} and K_1 as the fitting parameters. From the fitting, C_{max} gives the maximum molar concentration of adsorbates. The results of the fitting and the calculated $\Delta G°$ are summarized in Table 1.

Electrostatic interactions between MG and liposome

The experimental data obtained by the SHG measurement demonstrate that the electrostatic interactions between positively charged MG and the negatively charged POPG play a very important role in both the adsorption equilibrium of MG onto liposomes and the transport kinetics of MG across the liposome bilayer.

It is seen that the adsorption increases as the POPG content increases. The equilibrium constant has a 13-fold increase (Table 1) when the mole fraction of POPG increases from 25% to 100%. It follows that the negative adsorption free energy calculated by Eq. 8 increases as the PG content increases (Table 1). We also observed from the SHG measurement (Fig. 3) that there is no adsorption of MG on the 100% POPC liposome, which is a neutral liposome. This result indicates that the electrostatic interaction between cationic MG and anionic POPG is essential for adsorption to the POPG-POPC liposome surface. We also found that the number of adsorbates is determined by the amount of negatively charged POPG in the liposome. The maximum molar concentration of adsorbates, C_{max}, obtained from the fitting of adsorption isotherms scales linearly with the mole fraction of POPG in a liposome (Table 1). We can calculate the number of POPG molecules per adsorption site by [POPG]/C_{max}, where [POPG] is the concentration (moles per liter) of the lipid. We found it to be equal to 2.6 $\pm$ 0.1 regardless of the composition of the liposomes.

Finally, it is found that the POPG content of the liposome affects not only the adsorption but also the molecular transport across the bilayer. The decay constants k (s^{-1}) and dk/dc ($s^{-1}\,M^{-1}$) were found to be linearly dependent on the PG content of the liposomes (Fig. 6) as well as on the MG concentration (Fig. 5). Thus, we can obtain a simple empirical equation to describe the decay constant k:

$$k = a + bx_{PG}c, \tag{9}$$

where x_{PG} and c are the mole fraction of PG in the liposomes and the MG concentration, respectively, and a and b are constants obtained empirically. We see from Eq. 8 that the rate constant k (s^{-1}) is linearly dependent on x_{PG} and on MG concentration. This can be further illustrated in Fig. 6 that dk/dc scales linearly with the mole fraction of POPG of the liposomes as predicted by $dk/dc = bx_{PG}$.

TABLE 1 Fitting results of the adsorption isotherms shown in Fig. 7

Liposome POPG/POPC	K_1	C_{max} (μM)	$-\Delta G°$ (kcal/mol)
100:0	2.4 $\pm$ 0.7	4.7 $\pm$ 0.3	8.6 $\pm$ 0.2
75:25	0.67 $\pm$ 0.1	3.6 $\pm$ 0.5	7.8 $\pm$ 0.1
50:50	0.26 $\pm$ 0.09	2.4 $\pm$ 1.0	7.3 $\pm$ 0.2
25:75	0.18 $\pm$ 0.03	1.3 $\pm$ 0.5	7.1 $\pm$ 0.1

K_1 is the adsorption equilibrium constant given by Eq. 3, C_{max} is the maximum molar concentration of adsorbates, and $\Delta G°$ is the adsorption free energy.

CONCLUSIONS

Our experimental results demonstrate that the electrostatic interactions between the adsorbate cationic triphenyl organic molecule MG and the anionic POPG molecules present in the mixed POPG/POPC liposome play an essential role in both the molecular adsorption onto the liposome surfaces and the molecular transport across the liposome bilayers. We found that the more negatively charged was the POPG in the liposome, the larger was the extent of the adsorption and the more negative was the adsorption free energy. The concentration of adsorbed MG was found to scale linearly with the mole fraction of PG in the liposomes. We also found that the rate of the molecules crossing the liposome bilayers depends linearly on both the POPG content in the liposome and the MG concentration.

We thank the National Science Foundation and the Division of Chemical Science of the Department of Energy for their support.

REFERENCES

Aubard, J., P. Lejoyeux, M. A. Schwaller, and G. Dodin. 1990. Spectroscopy and kinetics of the interaction of ellipticinium derivatives with liposomes: influence of the aliphatic side chain on the binding mechanism. *J. Phys. Chem.* 94:1706–1711.

Bashford, C. L., B. Chance, J. Smith, and T. Yoshida. 1979. The behavior of oxonol dyes in phospholipid dispersions. *Biophys. J.* 25:63–85.

Buster, D. C., J. F. Hinton, F. S. Millett, and D. C. Shungu. 1988. ^{23}Na-nuclear magnetic resonance investigation of gramicidin-induced ion transport through membrane under equilibrium conditions. *Biophys. J.* 50:145–152.

Cafiso, D. 1989. Electron paramagnetic resonance methods for measuring pH gradients, transmembrane potentials and membrane dynamics. *Methods Enzymol.* 172:331–345.

Cafiso, D. S., and W. L. Hubbell. 1983. Electrogenic H^+/OH^- movement across phospholipid vesicles measured by spin-labeled hydrophobic ions. *Biophys. J.* 44:49–57.

Casals, C., E. Miguel, and J. Perez-Gil. 1993. Tryptophan fluorescence study on the interaction of pulmonary surfactant protein A with phospholipid vesicles. *Biochem. J.* 296:585–593.

Chakrabarti, A. C., I. Clark-Lewis, and P. Cullis. 1994. Influence of charge, charge distribution, and hydrophobicity on the transport of short model peptides into liposomes in response to transmembrane pH gradients. *Biochemistry.* 33:8479–8485.

Clarke, R. J. 1991. Binding and diffusion kinetics of the interaction of a hydrophobic potential sensitive dye with lipid vesicles. *Biophys. Chem.* 39:91–106.

Clarke, R. J. 1992. An adsorption isotherm for the interaction of membrane-permeable hydrophobic ions with lipid vesicles. *Biophys. Chem.* 42:63–72.

Clarke, R. J. 1993. A theoretical description of non-steady state diffusion of hydrophobic ions across lipid vesicle membranes including effects of ion-ion interactions in the aqueous phase. *Biophys. Chem.* 46:131–143.

Clarke, R. J., and H.-J. Apell. 1989. A stopped flow kinetic study of the interaction of potential-sensitive oxonal dyes with lipid vesicles. *Biophys. Chem.* 34:225–237.

Corn, R. M., and D. A. Higgins. 1994. Optical second harmonic generation as probe of surface chemistry. *Chem. Rev.* 94:107–125.

Eidelman, O., and Z. I. Cabantchik. 1989. Continuous monitoring of transport by fluorescence on cells and vesicles. *Biochim. Biophys. Acta.* 988:310–334.

Eisenthal, K. B. 1996. Liquid interfaces probed by second-harmonic and sum-frequency spectroscopy. *Chem. Rev.* 96:1343–1360.

Engelbert, H. P., and R. Lawaczeck. 1985. Isotopic light scattering of lipid vesicles. water permeation and effect of α-tocopherol *Chem. Phys. Lipids.* 38:365–379

Flewelling, R. F., and W. L. Hubbell. 1986. Hydrophobic ion interaction with membranes: thermodynamic analysis of tetraphenylphosphonium binding to vesicles. *Biophys. J.* 49:531–540.

Flewelling, R. F., and W. L. Hubbell. 1986. The membrane dipole potential in a total membrane potential model: applications to hydrophobic ion interaction with membranes. *Biophys. J.* 49:541–552.

Gabev, E., J. Kasianowicz, T. Abbott, and S. McLaughlin. 1989. Binding of neomycin to phosphatidylinositol 4,5-bisphosphate (PIP_2). *Biochim. Biophys. Acta.* 979:105–112.

Gennis, R. B. 1989. Biomembrane, Molecular Structure and Function. Springer-Verlag, New York

Haynes, D. H., and P. Simkowitz. 1977. 1-Anilino-8-naphthalenesulfonate: a fluorescent probe of ion and ionophore transport kinetics and transmembrane asymmetry. *J. Membr. Biol.* 33:63–108

Hope, M. J., B. Bally, G. Webb, and P. R. Cullis. 1985. Production of large unilamellar vesicles by a rapid extrusion procedure. *Biochim. Biophys. Acta* 812:55–65.

Kaiser, S., and H. Hoffmann. 1996. Transport of ions through vesicle bilayers. *J. Coll. Interfac. Sci.* 184:1–10.

Kakinoki, K., Y. Maeda, K. Hasegawa, and H. Kitano. 1995. Kinetics of binding processes of cytochrome C onto liposome surfaces. *J. Coll. Interfac. Sci.* 170:18.

Kerker, M. 1970. The Scattering of Light and Other Electromagnetic Radiation, 2nd ed. Academic Press, New York.

Ketterer, B., B. Neumcke, and P. Lauger. 1971. Transport mechanism of hydrophobic ions through lipid bilayer membranes. *J. Membr. Biol.* 5:225–245.

Kim, J., M. Mosior, L. Chung, H. Wu, and S. McLaughlin. 1991. Binding of peptides with basic residues to membranes containing acidic phospholipids. *Biophys. J.* 60:135–148.

Lasic, D. D. 1993. Liposomes from Physics to Application. Elsevier, Amsterdam.

Liu, Y., J. I. Dadap, D. Zimdars, and K. B. Eisenthal. 1999. Study of interfacial charge transfer complex on TiO_2: particles in aqueous suspension by second harmonic generation. *J. Phys. Chem. B.* 103: 2480–2486

Malmstein, M. 1995. Protein adsorption at phospholipid surfaces. *J. Coll. Interfac. Sci.* 172:106–115.

Marsh, D. 1990. CRC Handbook of Lipid Bilayer. CRC Press, Boca Raton, FL.

Mayer, L. D., M. J. Hope, and P. R. Cullis. 1986. Vesicles of various sizes produced by a rapid extrusion procedure. *Biochim. Biophys. Acta* 858: 161–168.

Mosior, M., and S. McLaughlin. 1991. Peptides that mimic the pseudosubstrate region of protein kinase C bind to acidic lipids in membranes. *Biophys. J.* 60:149.

Mosior, M., and S. McLaughlin. 1992. Binding of basic peptides to acidic lipids in membranes: effect of inserting alanine(s) between the basic residues. *Biochemistry.* 31:1767.

Noy, N., M. Leonard, and D. Zakim. 1992. The kinetics of interactions of bilirubin with lipid bilayers and with serum albumin. *Biophys. Chem.* 42:177–188.

Srivastava, A., and K. B. Eisenthal. 1998. Kinetics of molecular transport across a liposome bilayer. *Chem. Phys. Lett.* 292:345–351.

Sundeberg, S. A., and W. Hubbell. 1986. Investigation of surface potential asymmetry in phospholipid vesicles by a spin label relaxation method. *Biophys. J.* 49:553–562.

Terce, F., J.-F. Tocanne, and G. Laneelle. 1982. Interaction of ellipticine with model or natural membranes: a spectrophotometric study. *Eur. J. Biochem.* 125:203–207.

Voelker, D., and P. Smejtek. 1996. Adsorption of ruthenium red to phospholipid membranes. *Biophys. J.* 70:818–830.

Wallach, D. F. H., and R. J. Winzler. 1974. Evolving strategies and tactics in membrane research. Springer Verlag, New York.

Wang, H., E. C. Y. Yan, E. Borguet, and K. B. Eisenthal. 1996. Second harmonic generation from the surface of centrosymmetric particles in bulk solution. *Chem. Phys. Lett.* 259:15–20

Wang, H., E. C. Y. Yan, Y. Liu, and K. B. Eisenthal. 1998. Energetics and population of molecules at microscopic liquid and solid surfaces. *J. Phys. Chem. B.* 102:4446–4450.

Xiang, T. X., and B. D. Anderson. 1997. Permeability of acetic acid across gel and liquid crystalline lipid bilayers conforms to free-surface area theory. *Biophys. J.* 72:223–237.

Yan, E. C. Y., and K. B. Eisenthal. 1999. Probing the interface of microscopic clay particles in aqueous solution by second harmonic generation. *J. Phys. Chem. B.* 102:6056–6060.

Yan, E. C. Y., and K. B. Eisenthal. 2000. Effect of cholesterol on molecular transport of organic cations across liposome bilayers probed by second harmonic generation. *Biophys. J.* 79:898–903.

Yan, E. C. Y., Y. Liu, and K. B. Eisenthal. 1998. New method for determination of surface potential of microscopic particles by second harmonic generation. *J. Phys. Chem. B.* 102:6331–6336.

Zucker, S. D., W. Goessling, and J. L. Gollan. 1995. Kinetics of bilirubin transfer between serum albumin and membrane vesicles. *J. Biol. Chem.* 270:1074–1081.